Proceedings of MARTEC 2010
The International Conference on Marine Technology
11-12 December 2010, BUET, Dhaka, Bangladesh

NUMERICAL STUDY OF FREE SURFACE EFFECT ON THE FLOW AROUND SHALLOWLY SUBMERGED HYDROFOIL

Md. Ashim Ali[1] and Md. Mashud Karim[2]

[1]Department of Naval Architecture &Marine Engineering (NAME)
Bangladesh University of Engineering and Technology(BUET)
Dhaka-1000, Bangladesh
E-mail: ashim.name@gmail.com

[2]Department of Naval Architecture &Marine Engineering (NAME)
Bangladesh University of Engineering and Technology(BUET),
Dhaka-1000, Bangladesh
E-mail: mmkarim@name.buet.ac.bd

ABSTRACT

The wave generation due to the presence of a body moving at steady forward speed beneath a free surface has been the subject of extensive research work in marine hydrodynamics. In this study, the free surface effect on the flow around shallowly submerged hydrofoil is numerically computed. Finite Volume Method (FVM) based on Navier-Stokes equations is used for this purpose. The standard NACA 0012 hydrofoil section is used for ease of comparison with available experimental data. The k-ε turbulence model has been implemented to simulate turbulent flow past the foil surface. To get the free surface elevation, "Volume of Fluid" (VOF) method is incorporated in numerical simulation. Grid independency is checked using four grids of different sizes. To validate the computational results, the free surface wave generated by the flow around hydrofoil at submergence depth ratio h/c = 0.91 is compared with experimental results published by Duncan. The computed results show satisfactory agreement with the experimental measurements. Finally, free surface effects on wave profile are computed for six submergence depth ratios, h/c ranging from 0.911 to 4.0 *and maximum amplitude at two different Froude nos. (*F_n = 0.5672 and 0.70*)*

Keywords: Free Surface Effect, Hydrofoil, CFD, Viscous Flow, Wave Breaking, Volume of Fluid method.

1. INTRODUCTION

Numerical prediction of wave pattern, lift force and drag force of submerged hydrofoil has much importance to the researchers. The hydrodynamics of hydrofoils has become a matter of renewed interest in recent years because of their potentialities in the design of small craft. Such hydrofoils differ from conventional hulls in that they obtain their lift by hydrodynamic action rather than by hydrostatic buoyancy. In this regard they are closely related to planning surfaces and airfoils. When deeply submerged, in fact, the hydrofoil has a flow pattern which is identical to that of an airfoil of the same geometry moving at the same Reynolds number. It seems logical, therefore, to start any theoretical or experimental study of hydrofoils by using methods which are well known and widely utilized in aerodynamics. Duncan (1983) carried out experiments for NACA0012 for various submergence depth, angle of attack and velocity. He obtained free surface wave elevation, the breaking and non-breaking wave resistance of a two dimensional hydrofoil. Coleman (1986) tried to simulate the breaking process for the foil using finite-difference method by the application of an artificial pressure distribution on the free surface and a Kutta condition at the trailing edge. He showed rather phase-shifted and over predicted wave profile. Liu (1991) calculated the wave pattern for the foil using an NS solver with zero-equation turbulence model, but did not show good agreement with experiments. Hino (1993) introduced finite-volume method with an unstructured grid for free surface flow simulations. The method was based on Euler equations and showed good results.

The main objective of this research is to study the free surface wave generation for submerged hydrofoil at different submergence depths and observe the effect of submergence depth on maximum amplitude of generated wave. The numerical study is carried out using CFD software namely STAR CCM+.

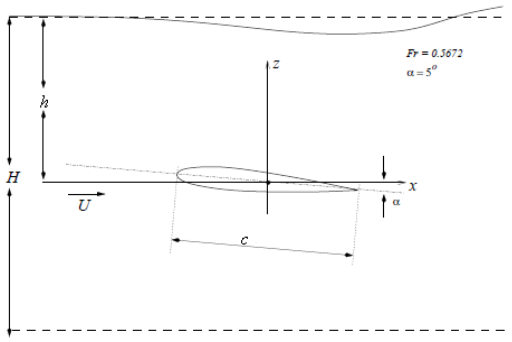

Figure 1: Geometry of flow past a hydrofoil.

2. MATHEMATICAL FORMULATION

The Navier-Stokes equations are the basic governing equations for a viscous, compressible real fluid. It is a vector equation obtained by applying Newton's Law of Motion to a fluid element and is also called the momentum equation. It is supplemented by the mass conservation equation, also called continuity equation. The instantaneous continuity equation and momentum equation for a compressible fluid can be written as:

$$\frac{\partial \rho}{\partial t} + \frac{\partial}{\partial x_j}\left[\rho u_j\right] = 0 \qquad (1)$$

$$\frac{\partial}{\partial t}\left(\rho u_i\right) + \frac{\partial}{\partial x_j}\left(\rho u_i u_j + p\,\delta_{ij} - \tau_{ji}\right) = 0 \qquad (2)$$

$$i = 1, 2, 3$$

If the fluid is Newtonian, then

$$\tau_{ij} = 2\mu S^*_{ij},$$

$$S^*_{ij} = \frac{1}{2}\left(\frac{\partial u_i}{\partial x_j} + \frac{\partial u_j}{\partial x_i}\right) - \frac{1}{3}\frac{\partial u_k}{\partial x_k}\delta_{ij} \qquad (3)$$

Where, S^* is the rate-of-strain tensor.

In the present study a submerged hydrofoil moving with a speed *U(t)* in calm water is considered as shown in Figure 1. A right-hand Cartesian coordinate system *o-xyz* is adopted with *x*-axis pointing forward, the *z*-axis pointing upward. The *x-y* plane is coincident with the undisturbed free surface. *c* is the chord length of hydrofoil. *h* is the distance between the center of the chord length and the free surface.

3. NUMERICAL SIMULATION

The Navier-Stokes equations are solved by using a fixed staggered grid. The basic algorithm is the two step projection method in which a time discretization of the momentum equation is broken up into two steps. In the first step, a velocity field is computed from incremental changes resulting from viscosity, advection, gravity and body forces. In the second step, the velocity field is projected onto a zero divergence vector field resulting into a single Poisson equation for the pressure field which is solved by using an incomplete Cholesky conjugate gradient solution technique.

To get the free surface elevation "Volume of Fluid" (VOF) method is used in numerical simulation. This method is pioneered by Hirt and Nichols (1981). The VOF technique provides a means of following fluid regions through an Eulerian mesh of stationary cells. The basis of the VOF method is the fractional volume of fluid scheme for tracking free surface boundaries. The governing equation in this method is given by:

$$\frac{DF}{Dt} = \frac{\partial F(\vec{x},t)}{\partial t} + \left(\vec{V} \bullet \nabla\right) F(\vec{x},t) = 0 \qquad (4)$$

Where F is defined whose value is unity at any point occupied by fluid and zero elsewhere. When averaged over a computational cell, it is equal to the fractional volume of the cell occupied by fluid. In particular, a unit value of F corresponds to a cell full of fluid, whereas a zero value indicates that the cell contains no fluid. Cell with F values between 0 and 1 contains a free surface. In addition to defining which cells contain a boundary, the F function can be used to define where fluid is located in a boundary cell.

For numerical study of turbulence, *k-ε* model is used. A *k-ε* turbulence model is a two-equation model in which transport equations are solved for the turbulent kinetic energy k and its dissipation rate ε. Various forms of the *k-ε* model have been in use for several decades, and it has become the most widely used model for industrial applications. Since the inception of the *k-ε* model, there have been countless attempts to improve it.

The standard *k-ε* model is a standard version of the two-equation model. The basic transport equations of which are:

$$\frac{d}{dt}\int_V \rho\, k\, dV + \int_A \rho\, k\left(v - v_g\right).da = \int_A \left(\mu + \frac{\mu_t}{\sigma_k}\right)\nabla k\,.\,da + \int_V \left[G_k + G_k - \rho\left((\varepsilon - \varepsilon_0) + Y_M\right) + S_k\right]dV \qquad (5)$$

$$\frac{d}{dt}\int_V \rho\,\varepsilon\, dV + \int_A \rho\,\varepsilon\left(v - v_g\right).da = \int_A \left(\mu + \frac{\mu_t}{\sigma_\varepsilon}\right)\nabla \varepsilon\,.\,da + \int_V \frac{1}{T}\left[\begin{matrix} C_{\varepsilon 1}\left(G_k + G_{nl} + C_{\varepsilon 3}G_b\right) - \\ C_{\varepsilon 2}\rho\left(\varepsilon - \varepsilon_0\right) + \rho\, Y_M + S_\varepsilon \end{matrix}\right]dV \qquad (6)$$

Where S_k and S_ε are the user-specified source terms. ε_0 is the ambient turbulence value in source terms, G_k is the generation of turbulence kinetic energy due to the mean velocity gradient, G_{nl} is the nonlinear production, G_b is the generation of turbulence kinetic energy due to buoyancy, Y_M represents the contribution of the fluctuating dilatation in compressible turbulence to the overall dissipation rate, $C_{\varepsilon 1}$, $C_{\varepsilon 2}$ and $C_{\varepsilon 3}$ are constant, σ_k and σ_ε are the turbulent Prandtle numbers for k and ε, respectively.

The turbulence kinetic energy, k is given by

$$k = \frac{3}{2}\left(U_{avg} I\right)^2$$

Where, U_{avg} is the mean flow velocity.
The turbulence intensity, I and the turbulence length l can be found from the following equations:

$$l = 0.07 \times L \text{ and } I = 0.16\left(Re\right)^{-\frac{1}{8}}$$

Also the turbulence dissipation rate, ε defined as:

$$\varepsilon = C_\mu^{\frac{3}{4}} \frac{k^{\frac{3}{2}}}{l}$$

The constants in Standard k-ε model are considered as:

$C_{\varepsilon 1} = 1.44$, $C_{\varepsilon 2} = 1.92$, $C_\mu = 0.09$, $\sigma_k = 1.0$ and $\sigma_\varepsilon = 1.3$

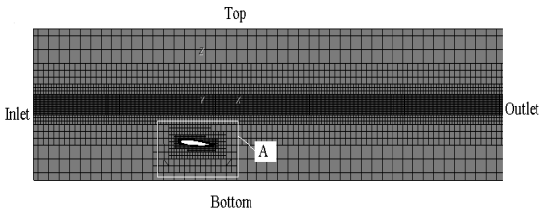

Figure 2: Mesh distribution in fluid domain.

CFD software package STAR CCM+ is used for numerical simulation. In this simulation, VOF method is employed for the free surface tracking. Figure 2 shows the fluid domain which is used for numerical simulation and Figure 3 is the close up view at hydrofoil which shows the mesh distribution around hydrofoil surface. To check the grid independency a numerical model set up with four different mesh sizes are used, which are partly shown in Figure 4. Trimmer meshing model is used to generate volume mesh in STAR CCM+. The general surface settings for all meshes are the same. The inlet is set as velocity Inlet, Outlet as pressure Outlet, top and bottom wall as slip wall so that there will be no friction. To get the wave profile, a refined region between z = 0.2 m and z = -0.2 m containing the free surface (z=0) is defined. Four grids namely Grid 1, Grid 2 Grid 3 and Grid 4 as shown in Figure 4 are used to check the grid independency. The coarse hexahedral mesh is refined to 0.1 m in Grid 1, 0.08 m in Grid 2, 0.05m in Grid 3 and 0.04 m in Grid 4 as shown in Table 1.

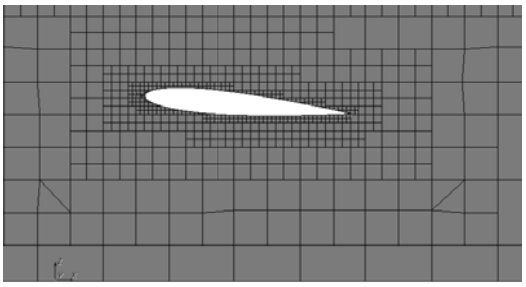

Figure 3: Close up views of A.

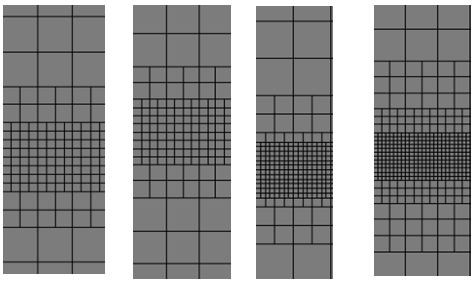

Figure 4: Mesh refinement.

Table 1: Grid specification

Grid no	Size of refined mesh
Grid 1	0.10 m
Grid 2	0.08 m
Grid 3	0.05 m
Grid 4	0.04 m

4. RESULTS AND DISCUSSIONS

As a test case, a simulation was carried out for NACA 0012 having h/c = 0.911 and Fn = 0.5672, Re = 1.7695 X 10^6 and angle of attack 5^0. To check grid independency, the wave profile is computed for different grids and plotted in Figure 5. From this figure it is seen that all grids make similar results with a little discrepancy. However, the refined Grid 4 is chosen for the simulation as it gives results very close to experimental ones. In Figure 6, the numerical result with Grid 4 is compared with the experimental results of Duncan(1983). Up to x/c = 4.0, the numerical results show good agreement with experimental results. After x/c = 4.0, the numerically calculated wave is gradually damped out but in case of

experimental results, the wave amplitude is observed nearly the same. However, the numerical results agree well with those of Muscari (2003) and Pascareli (2002).

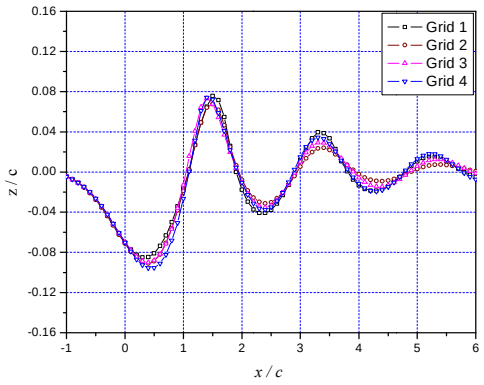

Figure 5: Grid independency

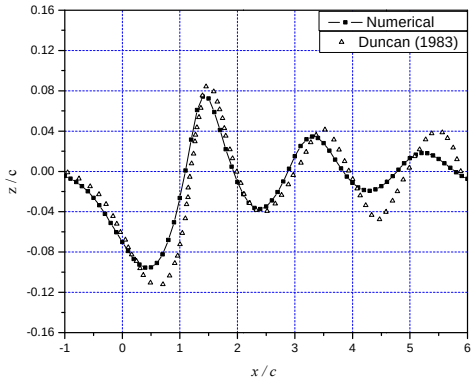

Figure 6: Comparison of Experimental and Numerical results

May be more refined mesh could give more accurate results but for the limitation of computer resources, Grid 4 is chosen here. Figures 7 to 10 show the convergence history of the numerical simulation with different grid sizes. Simulation is carried out using time step size of 0.05s. It is seen that the residual for all parameters is getting constant after 6000 iteration. With the decrease in the cell size, the fluctuation in residual value is getting higher. But as the decrease in the cell size makes the numerical results close to experimental results, the small cell size is chosen for further simulation.

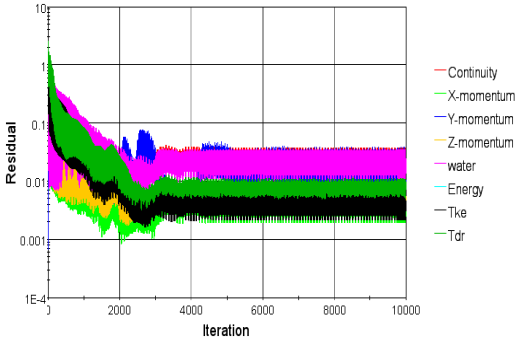

Figure 7: Convergence history for Grid 1.

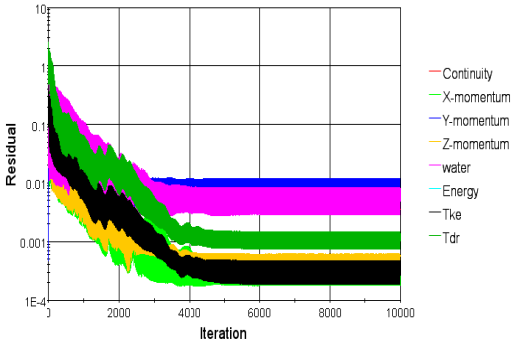

Figure 8: Convergence history for Grid 2

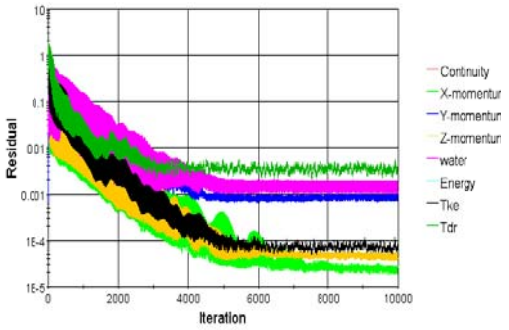

Figure 9: Convergence history for Grid 3.

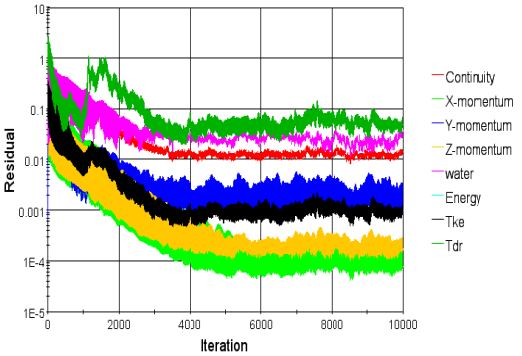

Figure 10: Convergence history for Grid 4.

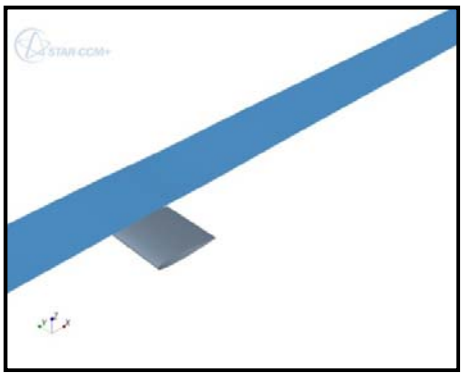

Figure 11: Visualization of free surface at t = 0.0s

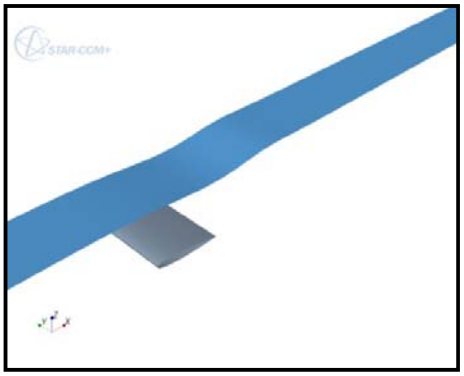

Figure 12: Visualization of free surface at t = 2.0s

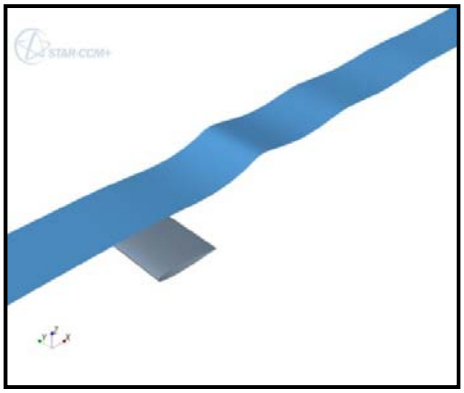

Figure 13: Visualization of free surface at t = 10.0s

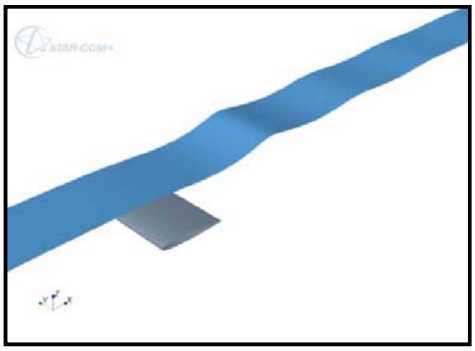

Figure 14: Visualization of free surface at t = 50.0s

Figure 11 to 14 shows the wave generation for a submerged hydrofoil having h/c = 0.911 at different times of the simulation. Figure 15 shows the effect of submergence depth ratio h/c on the free surface elevation. The rate of change in maximum amplitude is decreasing with increase in h/c. The variation of maximum amplitude with respect to h/c is shown in Figure 16. It is seen that the maximum amplitude increases exponentially with decrease in submergence depth ratio, h/c. It means that for small value of h/c, maximum wave amplitude, A_m is very large and there may be wave breaking on generated wave.

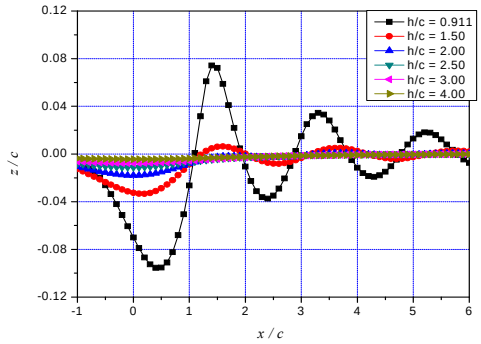

Figure 15: Effect of h/c on free surface elevation.

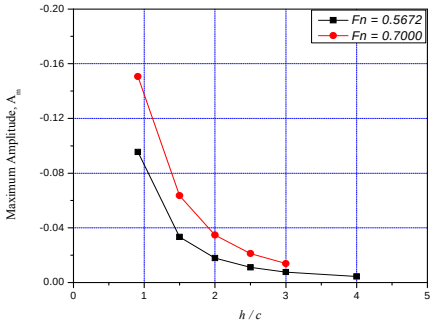

Figure 16: Effect of h/c on maximum wave amplitude.

Table 2: Force coefficients for hydrofoil at α=5°, F_n = 0.5672

Submergence depth ratio, h/c	Lift coefficient C_L	Drag coefficient C_D
0.91	0.6032519341	0.02192726918
1.50	0.5493059158	0.01405391004
2.00	0.5341051221	0.01186849736
2.50	0.5312077403	0.01301105693
3.00	0.5296801329	0.01120258588
4.00	0.5258696675	0.01115290634
Deep water (Experimental value)	0.5180	0.0113

Table 2 shows the lift and drag coefficients of hydrofoil at α=5° for different submergence depth ratios. It also shows the experimental values taken from the book by Abbott & Doenhoff (1959). As the submergence depth ratio increases, lift and drag coefficients decrease except the drag coefficient at *h/c* =2.5. At *h/c* =4 coefficients are almost close to the experimental values at deep water. So submergence depth ratio more than 4.0 can be treated as the deep water case and free surface effect becomes almost zero.

5. CONCLUSION

In the present work, finite volume method is used incorporating VOF method and *k-ε* turbulence model for simulation of the turbulent flow around shallowly submerged hydrofoil. From the above study, it can be concluded that the present method is successfully applicable to compute free surface wave generated by the hydrofoil moving beneath the surface. As the submergence depth ratio increases, the wave amplitude decreases. At the submergence depth ratio, *h/c* > 4.0, the effect of free surface vanishes. Similarly, the lift and drag coefficients decrease with increase in submergence depth ratio and become constant after *h/c* = 4.0. This implies that for submergence depth ratio greater than 4, shallow water effect does not exist and the deep water condition can be considered.

REFERENCES

[1] Abbott, I. H. and von Doenhoff, A. E., "Theory of Wing Sections," Dover Publications, New York, 1959.

[2] Coleman R. M.,"Nonlinear Calculation of Breaking and Non-Breaking Waves Behind a Two-Dimensional Hydrofoil", 16th Sym. On Naval Hydro. Berkeley, USA, July 1986.

[3] Duncan J. H., "The breaking and non-breaking wave resistance of a two-dimensional hydrofoil", J. Fluid Mech. Vol. 126, 1983.

[4] Hino T.,"A Finite-Volume Method with Unstructured Grid for Free Surface Flow Simulations", 6th Int. Conf. on Numerical Ship Hydro, Iwoa, USA, Aug. 1993.

[5] Hirt, C.W., Nichols, B.D. (1981), "Volume of fluid (VOF) method for the dynamics of free boundaries", *Journal of Computational Physics* 39 (1): 201-225.

[6] Liu H. and Ikehata M., "Computation of Free Surface Viscous Flow with High Reynolds Number around a Submerged Hydrofoil", 2nd Osaka Int. Colloquium on Viscous Fluid Dynamics in Ship and Ocean Tech., Japan, Sep. 1991.

[7] Muscari R, Di Mascio A (2003) A model for the simulation of steady spilling breaking waves. J Ship Res 47:13–23.

[8] Pascarelli. A , Iaccarino. G & Fatica. M, Proceedings of the Summer Program, Center for Turbulence Research. , 2002.